Development and field application of an automatic weld bead appearance inspection process using deep learning with welding conditions as parameters

Watanabe, Norihiro
Department of Marine Systems Engineering, Faculty of Engineering, Kyushu University : Doctoral course student

Yamasaki, Kento
Production Technology Section, Oshima Shipbuilding Co.,Ltd.

Gotoh, Koji
Department of Marine Systems Engineering, Faculty of Engineering, Kyushu University : Professor

Development and field application of an automatic weld bead appearance inspection process using deep learning with welding conditions as parameters.

Norihiro Watanabe*[1,2], Kento Yamasaki[2], Koji Gotoh[3]

1) Doctoral course student, Department of Marine Systems Engineering, Faculty of Engineering, Kyushu University
2) Production Technology Section, Oshima Shipbuilding Co.,Ltd.
3) Professor, Department of Marine Systems Engineering, Faculty of Engineering, Kyushu University
Email: n-watanabe@ma.osy.co.jp (*)

Abstract

This study explores the automation of welding inspection processes in shipyards by leveraging deep learning technologies to develop a system that aims to improve both efficiency and accuracy. We performed 90 horizontal fillet weld tests in a laboratory environment and 96 tests in a field environment on a T-shaped joint specimen, obtaining output logs from the welding machine during the welding process. We investigated deep learning computational methods and data preprocessing, introducing input data standardization and grid search for hyperparameters. As a result, the adjusted coefficient of determination for estimating leg length and undercut depth was improved. Next, we examined the frame size and the amount of frame shift for separating the input data were investigated, and the optimal values were identified that met practical criteria in a laboratory environment.
In addition, we conducted field tests using a simple welding carriage commonly used in shipyards to validate the applicability of our system in real-world environments. The results showed that the adjusted coefficients of determination for leg length and undercut depth estimation were 0.69 and 0.45, respectively, demonstrating the potential of our approach to improve production efficiency through automated weld quality inspection.
However, the study also identifies future challenges, including the need for more comprehensive training data, the incorporation of environmental data, and improvements in the estimation capabilities for various weld appearance features. This research serves as a step towards the automation of welding processes in the shipbuilding industry and provides directions for future research.

Keywords: Inspection of weld bead appearance, Deep learning, leg length, undercut depth, field tests

1. Study background

Automatic welding machines such as multi-electrode arc welding have been introduced in major domestic shipyards, achieving a certain degree of automation. However, visual inspection of weld appearance remains manual, time-consuming, and dependent on trained inspectors. As a result, defects may be missed, leading to rework and reduced production efficiency. Therefore, the development of an automated weld inspection system to reduce labor costs, ensure weld quality, and improve production efficiency is highly anticipated.

During the welding process at shipbuilding sites, as shown in Figure 1, simple welding carriages, line welders, and welding robots are typically operated as automated welding. An automated inspection system would maximize their effectiveness. Recently, deep learning has shown promise in estimating welding defects. It enhances learning capabilities by connecting neural networks in multiple layers to learn data patterns. While molt pool images provided highly accurate estimates [1-8], high camera costs and image stability issues due to welding fumes pose challenges. In addition, systems using bead shape images for estimation require images after slag removal, making real-time estimation difficult.

Given these challenges, system suitable for shipbuilding should estimate weld bead appearance using welding parameters rather than images. This study aims to develop and test a deep learning model using log data from welding power sources and fixed welding conditions as training data, as shown in Figure 2.

The initial focus was on improving the model's estimation accuracy if the model through hyperparameter search and frame settings. Field application experiments with a simple welding carriage validated the proposed method. The study focuses on "leg length" and "undercut depth", which are critical for joint strength and can be visually confirmed, targeting fillet welds joints produced by the single-pass process, commonly used in ship structures.

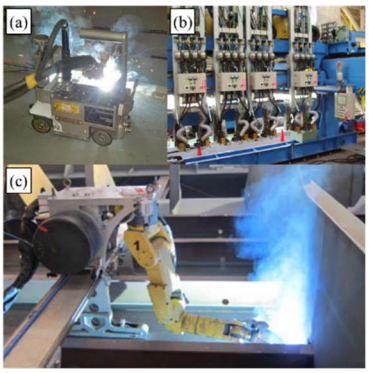

(a) Welding carriages, (b) line welders and (c) welding robots
Figure 1. Examples of automatic welding machines used in ship construction processes.

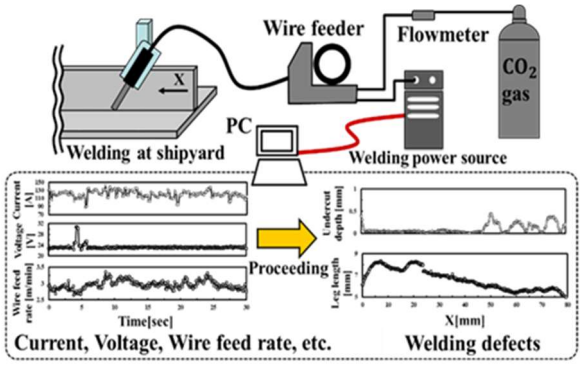

Figure 2. Inline welding inspection system.

2. Study method

2.1. Horizontal Fillet Welding Test and Acquisition of Weld Appearance Feature Data

To construct an automated weld defect inspection system, we conducted 90 horizontal fillet welding tests in a laboratory and 96 tests in a field environment. We collected output logs from the welding machine (current, voltage, wire feed speed) [9] and used a 2D laser displacement sensor (LJ-X8000 [10]) to obtain 3D coordinate data of the weld appearance. From these data, we extracted the distribution of leg length and undercut depth along the weld line. The horizontal plate in Figure 3 is referred to as “the main plate” and the vertical plate is called as it is.

This study focuses on estimating the features on the vertical plate side, where undercut depths greater than 0.5 mm occur more frequently and require repair. Due to insufficient learning data for the main plate side, we limited our estimation to the vertical plate side.

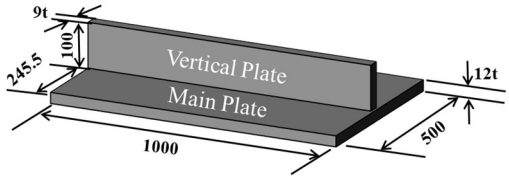

Figure 3. Test piece used for the Tee shaped-joint welding. (unit in mm)

2.2. Creation of Frames and Datasets

A frame is defined as "a section of welding machine log data and weld defect feature data segmented at regular intervals along the welding direction”. For example, with a weld length of 1,000 mm and frame lengths (F_L) of 10 mm with a frame shift (F_S) of 1 mm, 991 frame data points are created. In the lab environment, 90 weld tests generated 89,190 frames, with 87,995 valid data points after excluding missing values.

Welding machine output log data and weld defect feature data from the 90 test specimens were divided into training (70%), validation (15%), and test (15%) datasets. The allocation aimed to balance the current, voltage, welding speed, and defect feature quantities across the datasets.

2.3. Method for Estimating Leg Length and Undercut Depth Using Welding Machine Output Logs and Evaluation of Estimation Accuracy

We used MATLAB's Deep Learning Toolbox [11] to construct a back-propagation neural network (BPNN) to estimate for estimating leg length and undercut depth. The network consists of an input layer, hidden layers with hyperbolic tangent sigmoid functions, and a linear output layer. We used 12 optimization algorithms [12], including Levenberg-Marquardt Backpropagation [13] and Bayesian Regularization Backpropagation [14].

The input features were 16 statistics from the current, voltage, and wire feed rate of the time series data, for a total of 48 statistics and 4 fixed welding conditions to form a 52-dimensional feature vector. We trained the network weights with training datasets, adjusted them with validation datasets, and evaluated the accuracy on test data using the adjusted coefficient of determination (adjusted R^2 [15]). The training, validation, and testing process was repeated to optimize the network parameters. When treating the measured values of leg length and undercut depth as output values, the average value in each window is used for leg length and the maximum value in each window is used for undercut depth.

3. Results

3.1. Optimization of the Deep Learning Model in a Laboratory Environment

In order to improve the estimation accuracy of the deep learning model for practical applications, we standardized the feature vectors to a mean of 0 and a standard deviation of 1. This ensured a uniform influence of each feature vector on the estimation results. In addition, we performed a grid search to find the optimal settings for the hyperparameters: the number of neurons per layer (N), the number of hidden layers (H), and the optimization algorithm (A). We varied N from 1 to 10, H from 1 to 10, and selected A from 12 optimization algorithms in MATLAB.

Using standardized feature vectors and optimal hyperparameters, we trained the deep learning model. Figures 4(a) and 4(b) show the comparison between measured and predicted values of the test data for leg length and undercut depth, respectively. For leg length, N was set to 4, H was set to 7, and A was set to the Scaled Conjugate Gradient method [16]. For undercut depth, N was set to 4, H was set to 4, and A was set to Bayesian Regularization. The frame settings were F_L = 5 mm and F_S = 1 mm.

The adjusted coefficient of determination was approximately 0.68 for leg length and 0.58 for undercut depth. Although there was some agreement between the predicted and measured values, further optimization is needed.

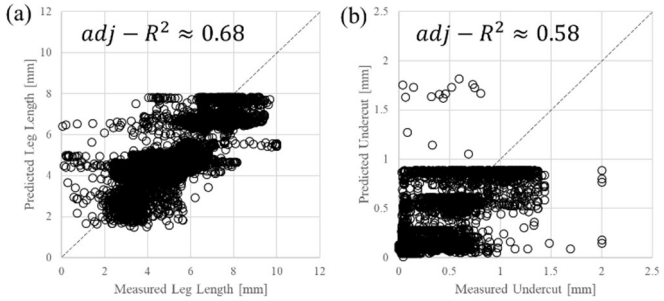

Figure 4. Result of standardized processing in addition to automatic search of neural network parameters.

Figure 5 shows the relationship between frame length (F_L) and the adjusted coefficient of determination for estimating leg length and undercut depth with a fixed F_S of 1 mm. For leg length, the adjusted coefficient reaches its maximum at F_L =100 mm, and for undercut depth, at F_L =10 mm.

Figure 6 shows the relationship between frame shift (F_S) and the adjusted coefficient of determination with a fixed frame length (F_L) of 100 mm for weld leg length and 10 mm for undercut depth. The maximum adjusted coefficient is obtained at F_S =50 mm for leg length and F_S =1 mm for undercut depth. However, increasing F_S reduces the number of training data. At F_L =100 mm and F_S =1 mm, the number of frames is 81,090, while at F_S =50 mm, it is reduced to 1710. The adjusted coefficient of determination is about 0.91 at F_S =1 mm, indicating high generalizability. Thus, the optimal frame shift for estimating the weld leg length is 1 mm.

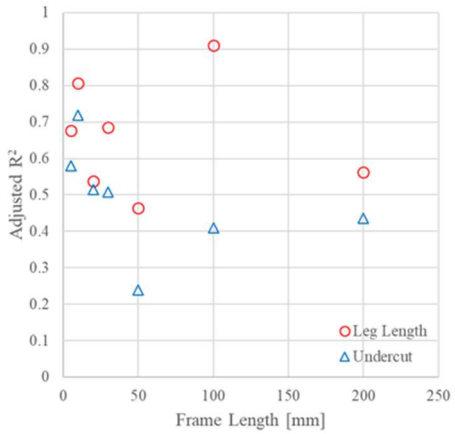

Figure 5. Adjusted R^2 versus frame length in leg length prediction and undercut prediction.

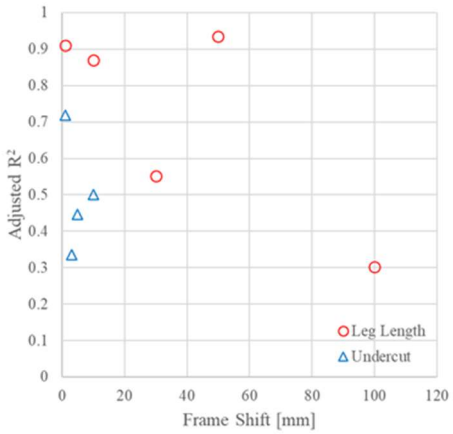

Figure 6. Adjusted R^2 versus frame shift in leg length prediction and undercut prediction.

The optimal values found are F_L =100 mm and F_S =1 mm for leg length, and F_L =10 mm and F_S =1 mm for undercut depth. Figures 7(a) and 7(b) show the comparison between measured and predicted values at these settings. The models showed relatively good agreement.

Figure 8(a) shows the comparison for weld leg length and Figure 8(b) for undercut depth for some frame numbers in the test data. The leg length model showed good agreement with the measured values, while the undercut depth model had significant discrepancies in some areas.

Upon completion of the deep learning model optimisation in the laboratory environment, we proceed to conduct field application experiments.

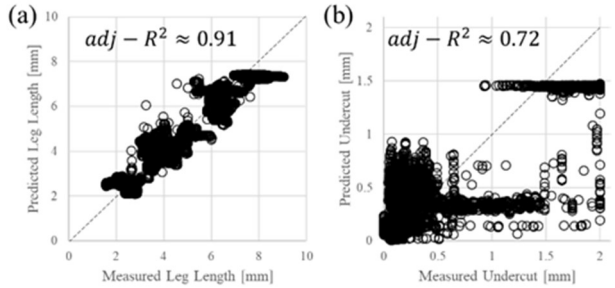

Figure 7. Comparison of measured and predicted (a) leg length and (b) undercut.

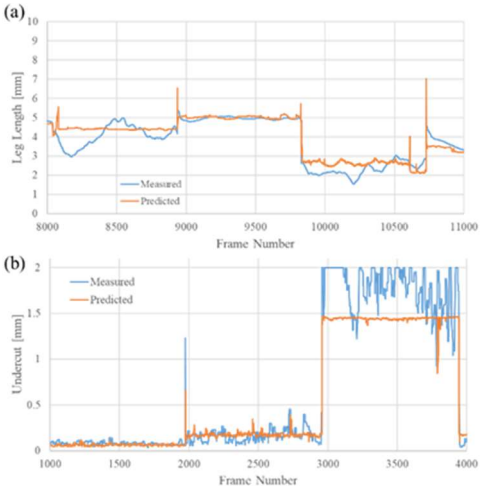

Figure 8. Comparison of measured and predicted (a) leg length and (b) undercut (the horizontal axis is the frame number).

3.2. Application Study in Field Environment

To advance the application study in a field environment, we conducted 96 horizontal fillet welding tests using a simple welding carriage, collecting welding machine output logs (current, voltage, wire feed speed, etc.). The equipment included a YD-500VR1 [17] (500A) welding power source, a Wel-Handy Multi II [18] welding carriage, and a metal-cored FCAW MX-200 [19] (wire diameter 1.4 mm) welding wire. Figure 9 shows the simple welding carriage, and the test specimen is the same as in Figure 3.

In Chapter 3, we intentionally induced welding defects by setting abnormal welding conditions. However, in this chapter, welding conditions were fixed to normal values to achieve stable welding, based on the assumption of practicality in the field. Defects like undercut or uneven welds were induced by external factors such as Zn-rich primer coating, derailing of the welding carriage, or reduced shielding gas flow. We conducted 96 tests: 24 with Zn-rich primer, 24 with the welding carriage derailed, 24 with reduced gas flow, and 24 under normal conditions. Figure 10 shows examples of weld beads under these conditions.

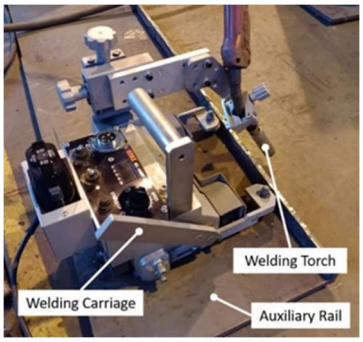

Figure 9. Welding carriage.

Figure 10. Weld bead appearances for each condition.

We applied the hyperparameter search method from Chapter 3, setting the number of neurons per layer (N) from 1 to 10, the number of hidden layers (H) from 1 to 10, and selecting the network weight update algorithm (A) from 12 optimization algorithms in MATLAB. The input data was standardized, and based on findings from Section 3.1, the frame length (F_L) and frame shift (F_S) were fixed at F_L = 100 mm and F_S = 1 mm for leg length estimation, and F_L = 10 mm and F_S = 1 mm for undercut depth estimation.

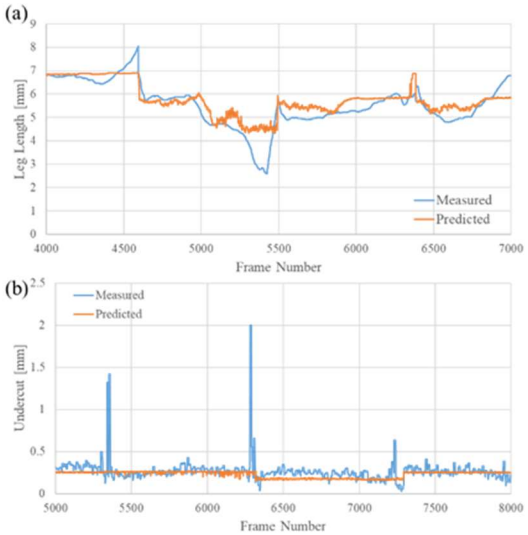

Figure 11. Comparison of measured and predicted weld (a) leg length and (b) undercut (the horizontal axis is the frame number).

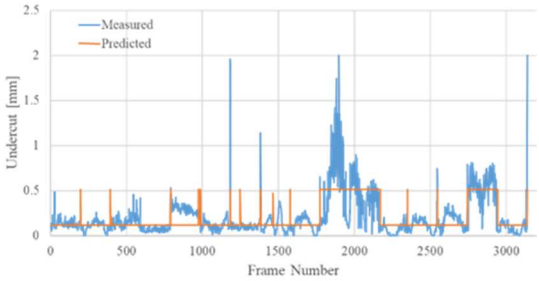

Figure 12. Comparison of measured and predicted undercuts under F_L = 10, F_S = 5 conditions (the horizontal axis is the frame number).

Figure 11(a) compares the measured and predicted leg length values, and Figure 11(b) compares measured and predicted undercut depth values. The optimized model showed partial agreement with leg length variations, but for undercut depth, the model failed to follow peaks around the 5400th, 6300th, and 7200th frame numbers.

We further examined undercut depth conditions by setting F_L = 10 mm and F_S = 5 mm. Figure 12 compares measured and predicted undercut depth values under these conditions, showing partial agreement with peaks.

Figure 13(a) compares measured and predicted leg length values, and Figure 13(b) compares measured and predicted undercut depth values for all test data. Optimization for leg length used N = 100, H = 1, and A with the BFGS Quasi-Newton backpropagation method [20]. For undercut depth, optimization used N = 1, H = 6, and A with the Resilient backpropagation method [21]. The adjusted coefficient of determination was 0.69 for leg length and 0.45 for undercut depth, indicating lower accuracy compared to the laboratory environment.

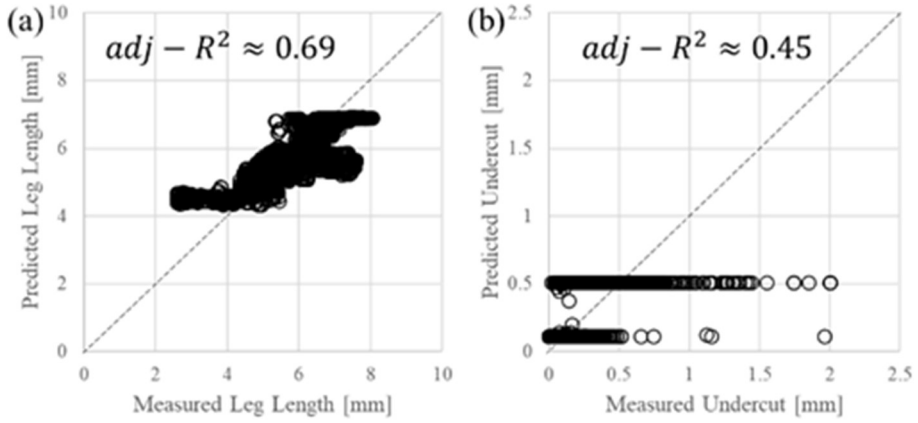

Figure 13. Comparison between prediction and experiment of (a) leg length (b) undercut on vertical plate side.

These results indicate that while the laboratory-optimized model showed some effectiveness, further refinement is needed for field application. The next step involves additional experiments and adjustments to improve the model's robustness and accuracy in real-world conditions.

4. Discussions

Improving the estimation accuracy for leg length can be achieved by accumulating more training data, enabling accurate estimations using only welding conditions. Estimating undercut depth is more challenging due to the difficulty in explaining localized features, resulting in lower sensitivity. The primary factors contributing to the lower adjusted coefficient of determination are as follows:

First, welding robots execute precise welds with accurate settings, while welding carriages require manual adjustments, leading to variability in aiming positions.

Second, uncertainty in external factors such as Zn-rich primer-coated steel, derailing of the welding carriage, and reduction in shielding gas flow affect welding defects. Estimation accuracy for undercut depth exceeding 0.5 mm was low, indicating that assumed external factors might have been insufficient.

Third, two-dimensional laser displacement sensors may struggle to capture reflective surfaces accurately, leading to missing values in measurement data.

Fourth, the algorithm calculating leg length and undercut depth from laser measurement data sometimes misidentifies the weld end, especially when undercut or spatter occurs. Improved identification and robust estimation methods for point cloud processing could enhance data quality.

Fifth, a small proportion of data exceeds the undercut depth threshold of 0.5 mm. The lack of defect data can lead to the model favoring normal data, reducing accuracy in predicting defects. Training the model with sufficient defect data is crucial for a more generalized deep learning model.

Achieving high estimation accuracy under shipyard welding conditions requires addressing the above challenges. Incorporating diverse environmental factors into the deep learning model, such as the roughness and shape of steel plate edges, the presence of oxidation films or slag, and environmental conditions like temperature, humidity, and wind speed, will be necessary for future applications.

5. Conclusions

Aiming to construct an automated welding inspection system applicable to shipyard environments, we addressed the following two major challenges. First, we optimized the deep learning model in a laboratory environment and determined the optimal values of F_L = 100 mm and F_S =1 mm for estimating the leg length on the vertical plate, and F_L = 10 mm and F_S =1 mm for estimating the undercut depth on the vertical plate. As a result, the adjusted coefficient of determination improved to 0.91 for leg length estimation and 0.72 for undercut depth estimation, confirming the potential applicability in the field.

Second, through experiments using a simple welding carriage widely used in shipyards, we estimated the leg length and undercut depth of the vertical plate during horizontal fillet welding. The results showed an adjusted coefficient of determination of 0.69 for leg length estimation and 0.45 for undercut depth estimation.

Future challenges include enriching the training data, incorporating environmental data, estimating other weld appearance features such as overlap and pits, and investigating other types of joints like butt joints and multi-layer welds.

Acknowledge

The authors would like to express their deepest gratitude to Yongyi Feng, a master's student in the Graduate School of Engineering, Kyushu University, for his deep cooperation in this research.

References

[1] Kasano, K., Ogino, Y., Fukumoto, S., Asai, S.: Study on welding phenomena observation method based on arc and moltenpool light emission characteristics in visible and infrared wavelength region – Development of image sensing technology for in-process welding monitoring technology -, Journal of The Japan Welding Society, Vol. 38 No.2, pp. 103-113, 2020 (in Japanese).

[2] Kasano, K., Ogino, Y., Fukumoto, S., Asai, S., Sano, T.: Observation of welding phenomena with blowholes for detection of welding defects – Development of in-process welding monitoring technology with image sensing technology -, Journal of The Japan Welding Society, Vol. 38 No.3, pp. 173-182, 2020 (in Japanese).

[3] Kasano, K., Ogino, Y., Sano, T., Asai, S.: Study on Practical Application for In-process Detection Method of Blowholes, Journal of The Japan Welding Society, Vol. 39 No.4, pp. 334-346, 2021 (in Japanese).

[4] Nitta, S., Ogino, T., Asai, S.: In-process monitoring of weld quality in thin plate lap welding by using image sensing, Journal of The Japan Welding Society, Vol. 38 No.2, pp. 114-124, 2020 (in Japanese).

[5] Takenaka, R., Aoyama, K., Oizumi, K.: Application of Machine Learning in Image Classification of Weld Bead Quality, Conference Proceedings The Japan Society of Naval Architects and Ocean Engineers, Vol. 28, pp. 253-257, 2019S-GS7-1, 2019 (in Japanese).

[6] Z. Zhang, G. Wen, S. Chen, "Weld image deep learning-based on-line defects detection using convolutional neural networks for Al alloy in robotic arc welding." Journal of Manufacturing Processes, Vol. 45, pp. 208-216, 2019.

[7] C. Xia, Z. Pan, Z. Fei, S. Zhang, H. Li, "Vision based defects detection for Keyhole TIG welding using deep learning with visual explanation." Journal of Manufacturing Processes, Vol. 56, pp. 845-855, 2020.

[8] R. T. Martínez, G. A. Bestard, A. M. A. Silva, S. C. A. Alfaro, "Analysis of GMAW process with deep learning and machine learning techniques." Journal of Manufacturing Processes, Vol. 62, pp. 695-703, 2021.

[9] Morihira, N., Watanabe, N., Gotoh, K.: Fundamental Study of Automatic Inspection of Weld Bead Appearance by Machine Learning, Conference Proceedings The Japan Society of Naval Architects and Ocean Engineers, Vol. 28, pp. 259-260, 2019S-GS7-2, 2019 (in Japanese).

[10] https://www.keyence.co.jp/products/measure/laser-2d/lj-x8000/models/lj-x8000/, (accessed June 27, 2024).

[11] https://jp.mathworks.com/products/deep-learning.html，(accessed June 27, 2024).

[12] https://jp.mathworks.com/help/deeplearning/ug/train-and-apply-multilayer-neural-networks.html ，(accessed June 27, 2024)

[13] https://jp.mathworks.com/help/deeplearning/ref/trainlm.html，(accessed June 27, 2024)

[14] https://jp.mathworks.com/help/deeplearning/ref/trainbr.html，(accessed June 27, 2024)

[15] https://jp.mathworks.com/help/stats/coefficient-of-determination-r-squared.html，(accessed June 27, 2024)

[16] https://www.mathworks.com/help/deeplearning/ref/trainscg.html, (accessed July 8, 2024)

[17] https://content.connect.panasonic.com/jp-ja/fai/file/6825，(accessed June 27, 2024)

[18] https://www.koike-asia.com/Home/portable_machines/Wel-Handy_Multi_II?QUERYSTRING=WEL+Handy+multi+II，(accessed June 27, 2024)

[19] https://www.kobelco.co.jp/english/welding/files/handbook.pdf，(accessed June 27, 2024)

[20] https://www.mathworks.com/help/deeplearning/ref/trainbfg.html, (accessed July 8, 2024)

[21] https://www.mathworks.com/help/deeplearning/ref/trainrp.html, (accessed July 8, 2024)